International Journal of Scientific Research in Engineering and Management (IJSREM)
Volume: 09 Issue: 09 | Sept - 2025 SJIF Rating: 8.586 ISSN: 2582-3930

Non-Destructive Image Processing Methodology for Monitoring Corrosion in Concrete Reinforcement

Nishant Kumar[1], Prof. Satya Prakash[2]

[1]*Department of Civil Engineering, Sharda University, Greater Noida.*
[2]*Department of Civil Engineering, Sharda University, Greater Noida*

---***---

Abstract - Corrosion of reinforcement bars (rebars) is one of the most critical factors affecting the durability and safety of reinforced concrete (RC) structures. Conventional inspection techniques, such as half-cell potential testing, though reliable, are time-consuming, invasive, and provide limited spatial resolution. This study presents a non-destructive, automated approach for corrosion assessment using digital image processing algorithms implemented in Python with OpenCV. High-resolution images of rebars were pre-processed through resizing, blurring, grayscale conversion, thresholding, and contour detection, followed by polygon-based masking and color analysis to accurately quantify corroded regions. Validation was carried out against half-cell potential measurements (ASTM C876) across 20 reinforcement samples. Results demonstrated strong agreement between the two methods: corrosion levels ranged from 0.46% (-194 mV, low probability) to 97.53% (-610 mV, high probability), with consistent correlation across low, moderate, and severe damage ranges. The image processing algorithm achieved 100% true positive detection with no false classifications, while providing the added advantage of spatial visualization of corrosion patterns. The findings confirm that image-based assessment can complement traditional electrochemical techniques, improving diagnostic accuracy and efficiency. This approach offers a scalable, cost-effective, and non-invasive tool for structural health monitoring, with significant potential for integration into predictive maintenance and life-cycle management of RC structures.

***Key Words*:** Digital Image Processing; Corrosion Detection; Reinforced Concrete; Half-Cell Potential; Structural Health Monitoring; Non-Destructive Testing; Python Algorithms.

1.INTRODUCTION

Corrosion is the process of a material eroding attributable to chemical or electrochemical interaction of the environments, leading to material mass loss over some time. Concrete and reinforcing bars are constituents of Reinforced Cement Concrete (RCC) where concrete withstands the compressive strength and the reinforcing bars govern the tensile strength. Since corrosion is responsible for losing strength and is inextricably tied to a structure's long-term viability. Most of the structures today are made of reinforced bars. The reinforcing bars used in RCC structures should be good enough to bear tensile strength. When the corrosion starts on the one region of the bars the chances of getting corrosion on the other side of the bars get increased. Due to the rapid deterioration process involved, serviceability criteria design using reinforced bars gets compromised. The corrosion of steel bars induces the concrete to swell, and triggers scaling and fissures in the concrete, resulting in catastrophic events due to compromised performances through structural deterioration [1]. The tendency of a metal to corrode is governed by its microstructures, its composition as generated during alloying, or the temperature developed during manufacturing for the deformation of a single metal surface. It would be more pragmatic to prevent corrosion instead of endeavouring to eliminate it. corrosion mechanisms can be as diversified as the environments to which a substance is exposed, which makes them harder to comprehend. However, it can be controlled simply by understanding the mechanisms of a reaction involved in the process. National Association of Corrosion Engineers (NACE) studied the impact faced by corrosion on the global economy and concluded that the estimated cost of corrosion is about 2.5 trillion US$ which is equivalent to 3.4% of the GDP of 2013. The study also revealed that the saving costs can be increased between 15% to 35% of total cost if different corrosion management and controlling practices are followed [2].

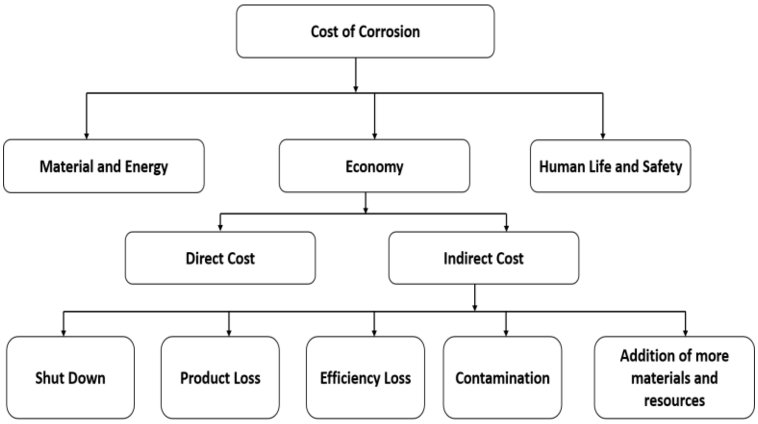

Fig -1: Cost of Corrosion [3-5]

The cost of corrosion becomes a burden due to its impacts on the economy, the safety of human life and material resources and energy. Furthermore, the direct and indirect corrosion costs are increased due to ignoring corrosion which adds up to the economic loss for any country. The cost of corrosion as shown in Figure 1 comprises the economic loss and safety of human life [6]. In Reinforced structures, trillions of dollars have been invested in the control of corrosion. Various non-destructive testing (NDT) techniques have been developed and employed to detect and assess corrosion in reinforcement bars. These techniques include but are not limited to electromagnetic methods like ground-penetrating radar (GPR), electrical resistivity measurements, half-cell potential mapping and ultrasonic testing. Detecting corrosion in reinforcement bars using image processing techniques represents a significant advancement in the field of structural health monitoring and maintenance of concrete structures. Traditional methods for assessing corrosion in reinforcement bars often rely on invasive or time-consuming procedures, making them less efficient for large-scale evaluations. However, the integration of image processing into corrosion detection offers a non-destructive and more accessible means to identify and analyze the extent of corrosion within these bars.

Corrosion is the inevitable degradation of steel influenced by numerous environmental parameters such as acid, moisture, etc. making it phenomenon more complex. The reactivity of the metal, the presence of inclusions, the availability of oxygen, humidity, gases such as Sulphur dioxide and carbon dioxide, and the availability of electrolytes are all factors that induce corrosion. While interlinked capillary's porosity makes it very difficult for chloride ions, oxygen and moisture to permeate concrete fractures and gives a more direct route to react with reinforced bar thus increasing the probability of corrosion [7-11]. Figure 2 explains the corrosion mechanism of reinforced concrete structure.

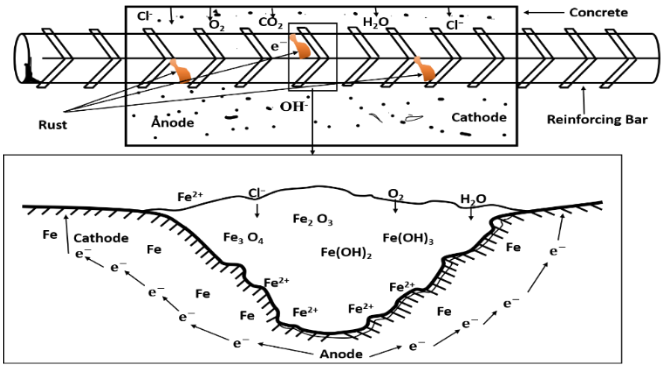

Fig -2: Corrosion Mechanism

The performance of RC structures diminishes as concrete structures deteriorate due to adverse climatic conditions, and the untimely disintegration of structures before the periodic maintenance life is a primary issue for engineers and researchers. The rate at which structures degrade is influenced by the conditions of exposure and the intensity of maintenance. Corrosion, which is triggered by chemical or electrochemical responses, seems to be the most prevalent cause of RC structure deterioration. It is primarily governed by chloride ingress and RC structure carbonation depth. Carbonation and infiltration of chloride ions are the two most common causes of rebar corrosion in concrete constructions. Corrosion of RC structures begins when chloride ions pierce concrete beyond the predefined threshold or when carbonation depth surpasses concrete cover.

If corrosion commences in concrete structures, it proceeds and diminishes the structures' service life, and the pace of corrosion has an impact on the remaining serviceability of RC structures [12]. Nevertheless, these extreme environments promote reinforcement corrosion unless the requisite concentrations of oxidative degradation are accessible at the rebar level in concrete structures. Corrosion of steel bars is the leading cause of concrete construction failure, with approximately two tonnes of concrete used per capita by the global population each year. As a consequence, it has been identified that long-lasting constructions will minimize cement use. Corrosion can significantly impair the strength and life of structures, and contaminants from the atmosphere can permeate through the concrete cover and induce corrosion of steel in humid situations. The cathode and anode are formed in various locations of the same reinforcing bar. Whenever the corrosive process is initiated, the section is degraded in the anodic region. The iron gets transformed into ferrous ionic species, which also are transferred from the anode to the cathode. These regions on the reinforcement bar exhibiting positive electrochemical potential serve as cathode material using moisture, reducing oxygen and devouring electrons from the anode to form hydroxyl ions. Inside the electrochemical system, the steel bars act as conducting materials, whereas the concrete solution functions as the electrolytic medium whereby the ions migrate.

Digital image processing, involving the use of algorithms executed by digital computers, serves as a pivotal tool for manipulating digital images. The process entails applying various operations to images, generating outputs with specific characteristics associated with the image. Its versatility allows for multiple applications, one of which is the detection of corrosion, the focus of our study. Images captured by cameras often lack clarity, necessitating image modifications prior to processing to ensure clarity and precision in the results obtained.

In our context, the primary aim is to detect corrosion within these images. This necessitates pre-processing steps to enhance image quality and enable unambiguous detection of corroded regions. The initial image might suffer from issues such as unclear details, noise, or variations in illumination. Consequently, our methodology involves a series of steps to rectify these issues. These steps encompass resizing the image to an optimal resolution, blurring to reduce noise and sharpen features, converting to grayscale for simplified processing, and thresholding to segment the corroded regions effectively.

The modification process is crucial to improve the image's suitability for corrosion detection. This is achieved through algorithmic manipulations facilitated by the Python programming language, leveraging libraries like OpenCV and NumPy. OpenCV provides a diverse set of tools for image processing tasks, while NumPy aids in numerical computations, both contributing significantly to the efficiency and accuracy of the algorithm.

Ultimately, the goal is to enable a more precise and automated identification of corroded areas within images. By addressing issues of image clarity and quality through tailored image processing techniques, we aim to enhance the reliability and effectiveness of corrosion detection methodologies in industrial and structural analysis applications.

International Journal of Scientific Research in Engineering and Management (IJSREM)
Volume: 09 Issue: 09 | Sept - 2025 SJIF Rating: 8.586 ISSN: 2582-3930

2. METHODOLOGY

Stage 1: Data Collection

Proper lighting conditions play a pivotal role in image capture, demanding uniformity and adequacy to avoid shadows or glare while ensuring detailed depiction. Direct sunlight, known to cause overexposure, should be circumvented. Moreover, image size and resolution must strike a balance; images should be detailed enough to retain necessary information without being excessively large, optimizing storage. High resolution becomes imperative for preserving clear and sharp details within the image. Simplicity in the background is equally crucial, serving to eliminate distractions and facilitate the distinction of the object of interest from the surroundings. A non-distracting background aids in focusing on the primary subject, enhancing the overall clarity and relevance of the captured image. Figure 3 explains the detailed methodology.

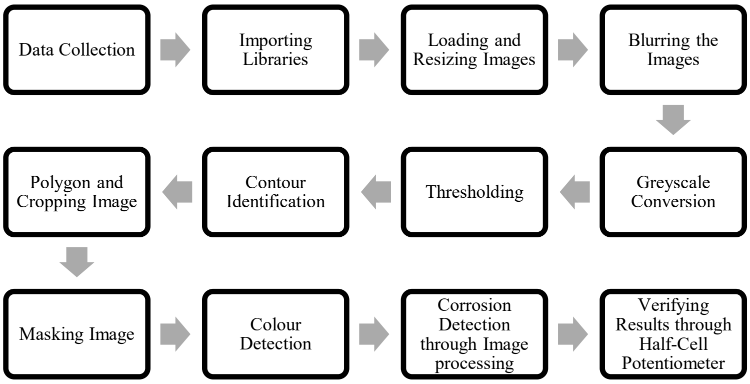

Fig -3: Digital Image Processing Algorithm

Stage 2: Loading and Resizing Image

Excessively high image resolution often leads to prolonged processing times and increased memory consumption. To mitigate this, resizing the image to a lower resolution can significantly enhance processing speed. Maintaining the original aspect ratio during resizing proves crucial, ensuring proportional adjustments and preserving the image's proportions. This approach facilitates faster processing; as smaller-sized images are more expediently handled compared to their larger counterparts.

Stage 3: Blurring the Image

Blurring an image holds significant importance within image processing due to multiple advantageous aspects:

1. Reducing Noise: Images often contain unwanted artifacts or noise that can disrupt the image analysis process. Blurring serves as a method to mitigate this noise, enabling a clearer identification of crucial features within the image.

2. Smoothing Edges: Sharp edges in an image sometimes hinder feature detection or accurate measurements. Blurring aids in smoothing out these edges, facilitating easier detection and measurement of features, thereby enhancing the analysis process.

3. Removing Unnecessary Details: Images might contain extraneous details that hold no relevance to the specific analysis being conducted. Blurring proves effective in eliminating such irrelevant details, enabling a focused analysis solely on the pertinent parts of the image.

Stage 4: Grayscale Conversion

A grayscale image is basically the representation of pixels based on their intensity. In other words, each pixel in a grayscale image is represented by a single value that ranges from 0 (black) to 255 (white), with values in between representing various shades of grey. Grayscale images are often used in image processing tasks because they are simpler to work with than full-colour images, and many image processing algorithms can be applied directly to grayscale images.

Stage 4: Thresholding

The conversion of a grayscale image into a binary image results in pixels having only two potential values: black or white. Setting the threshold value to 0 dictates that any pixel value below 0 becomes black, while values above 0 turn white. Thresholding plays a critical role in converting grayscale images into binary representations, thereby simplifying the segmentation of corroded and non-corroded regions. Three principal approaches were employed in this study. Global thresholding applies a single intensity value across the entire image, offering computational efficiency but limited adaptability under varying illumination conditions [13]. Otsu's method improves separation by selecting an optimal threshold that minimizes intra-class variance, making it effective for images with fluctuating contrast levels. Adaptive thresholding further enhances performance in non-uniform lighting by calculating localized thresholds based on statistical properties such as mean, Gaussian weighting, or median filtering, thereby enabling more precise segmentation of corrosion-prone areas [14-16]. Together, these methods ensure robust detection by balancing computational simplicity with accuracy across diverse imaging conditions.

Stage 5: Contour Identification

Contours are the boundaries of objects or regions in an image. This function returns two values: contours, which is a list of all the contours found, and hierarchy, which is a hierarchical representation of the contours. The contours are drawn in red colour with a thickness of 2 pixels.

Stage 6: Polygon and Cropping an Image

The boundaries of the image captured are set through demarking a polygon on the image captured and subsequently the image is cropped. The polygon will help us for detecting the corrosion in the interested area even if there is an unwanted background that affect the detection of corrosion such as shadow or any colour which looks like the corrosion. As we know that this method of image processing is based on colours so without the use of this technique, the program will automatically select the non-steel area having red colour. Through python programming the area of the selected polygon is calculated. This total area is important in calculating the total corroded area on the steel reinforcement.

Stage 7: Masking an Image

The function of this mask is to hide the unwanted or the uninterested part of the image which in this case is the area beyond the drawn polygon. The mask region is represented with black colour. It has to be noted that the mask will efficiently cover or remove all the uninterested area by transforming that particular area in to black colour.

Stage 8: Colour Detection

As we know that the corroded part or the rust has a reddish brown colour appearance. Through programming we can calculate the area of red region by counting the number of pixels having values greater than Zero which in our case is the white pixels.

Stage 9: Corrosion Detection

The percentage of corrosion is calculated based on the total area of the polygon drawn which includes the total number of white plus black pixels and the area of red area which counts the number of corroded pixels.

Stage 10: Verifying Results through Half Cell Potentiometer

Half-cell Potentiometer testing is done in accordance with ASTM C876 standards. This method involves measuring the potential value on the concrete surface, where the positive pole voltmeter connects electrically to the rebar, while the other pole links to a reference electrode. The potential difference is measured and subsequently assessed to determine the risk of corrosion within the embedded steel in the RC members [17].

3. RESULTS & DISCUSSION

Figure 4 displayed below illustrates the initial samples utilized for both the Half Cell Potential Experiment and as input for the Algorithm. The presence of green coloration in each sample denotes the polygon drawn by the user, indicating the specific location where the electrode was employed during the half cell potential test. This polygon's significance lies in guiding the Python program to execute precisely at that particular location.

The Python program is executed twice. Initially, the program is executed to detect the corrosion percentage precisely at the electrode location. Subsequently, the code is executed for the entire rebar. Notably, the obtained results differ as corrosion is non-uniform along the length of the rebar.

The derived results from these samples are compiled into a table, accompanied by the outcomes from the half-cell potential test. This comparative presentation facilitates an easy understanding of the correlation between the results obtained from the half-cell potential test and the corresponding outcomes subsequent to the Python program's execution. This tabulated representation aids in comprehending and analyzing the correlation between the experimental results and the computational findings obtained through Python programming.

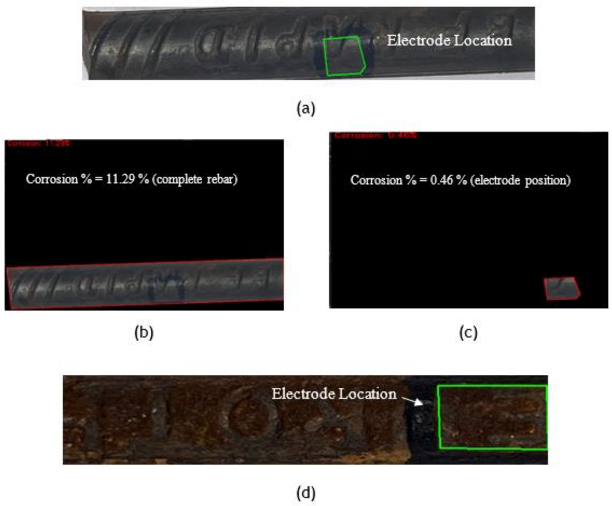

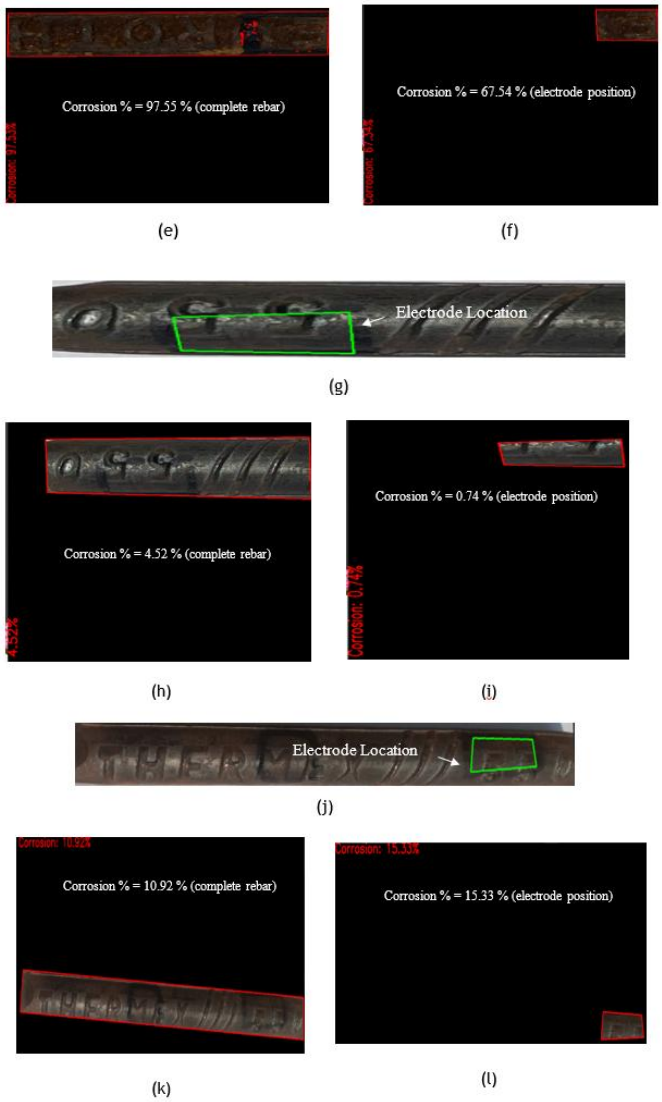

Fig -4: Reinforcement images (a) sample 1 (b) percentage of corrosion in sample 1 – whole steel bar (c) percentage of corrosion in sample 1 – electrode location (d) sample 2 (e) percentage of corrosion in sample 2 – whole steel bar (f) percentage of corrosion in sample 2 – electrode location (g) sample 3 (h) percentage of corrosion in sample 3 – whole steel bar (i) percentage of corrosion in sample 3 – electrode location (j) sample 4 (k) percentage of corrosion in sample 4 – whole steel bar (l) percentage of corrosion in sample 4 – electrode location

A total of 20 reinforcement bars were taken for the study and Table 1 discusses the readings from Half Cell Potentiometer test and the results given by the image processing.

International Journal of Scientific Research in Engineering and Management (IJSREM)
Volume: 09 Issue: 09 | Sept - 2025 SJIF Rating: 8.586 ISSN: 2582-3930

Table -1: Half-cell potentiometer vs Image processing results

Sample no	Half-cell potential Experiment Values(-mV)	% corrosion where the electrode is applied (algorithm results)	% corrosion for the whole rebar (algorithm results)	% chance of corrosion activity
1	194	0.46	11.29	10
2	610	67.34	97.53	90
3	187	0.74	4.52	10
4	189	15.33	10.29	10
5	594	84.21	89.32	90
6	654	83.22	87.23	90
7	354	65.22	88.31	90
8	210	35.31	44.74	50
9	280	37.31	45.44	50
10	397	68.21	79.61	90
11	616	79.31	88.41	90
12	132	0.54	1.14	10
13	115	0.55	1.03	10
14	233	35.31	44.21	50
15	237	37.31	49.21	50
16	312	41.44	47.21	50
17	415	67.31	71.21	90
18	437	72.14	81.44	90
19	514	77.34	85.23	90
20	632	81.21	89.22	90

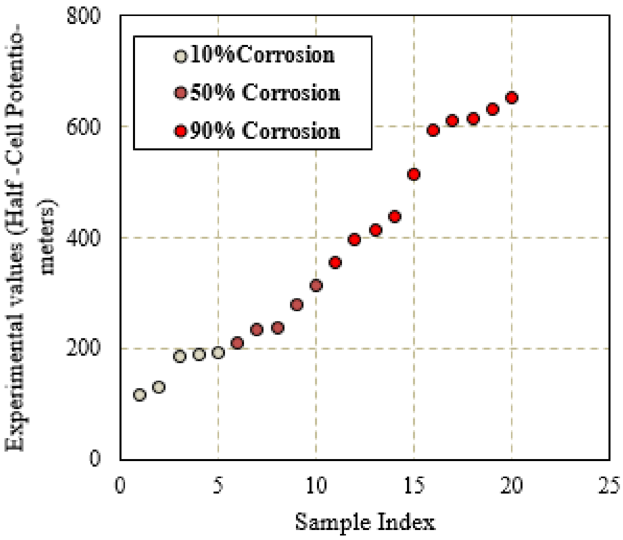

Fig -5: Corrosion result through experimental setup

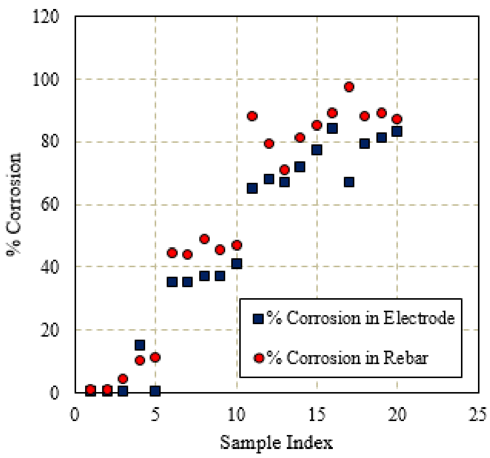

Fig -6: Corrosion result through image processing

As evident from the above table and Figure 5 and Figure 6 the results of corrosion percentage obtained through image processing are comparable with the experimental results obtained by half-cell potentiometer test. The results assembled from image processing offer a visual representation of corrosion patterns, enabling a comprehensive understanding of the distribution and severity of corroded regions along the reinforcement. This approach not only provides qualitative insights but also quantifies the corrosion percentage, facilitating a quantitative assessment akin to the traditional methods employed in the half-cell potential test. The confusion matrix shown in Figure 7 and Figure 8 also confirms that the model is running successfully and there are no True Negative (TN), False Positive (FP), False Negative (FN) within the model and all the results are indicating True Positive (TP) values.

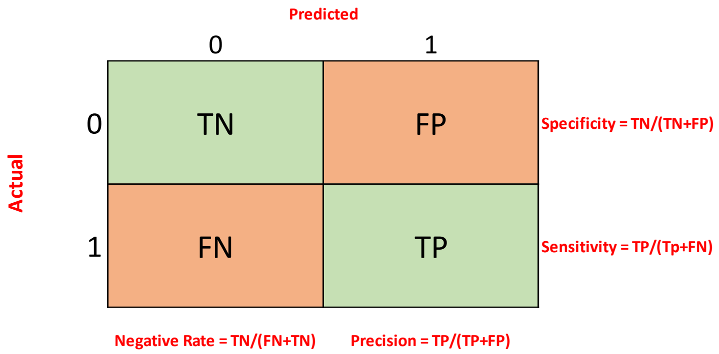

Fig -7: Confusion Matrix

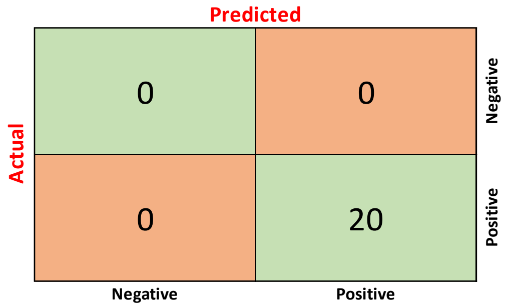

Fig -8: Confusion Matrix True Positive

The results derived from the image processing algorithm revealed a strong agreement with conventional half-cell potential measurements, demonstrating the reliability of digital approaches in corrosion quantification. For instance, Sample 1 showed 0.46% corrosion at the electrode location and 11.29% along the complete rebar, corresponding well with a half-cell potential of -194 mV, which indicated a low (10%) probability of corrosion. Conversely, Sample 2 exhibited extensive degradation, with 67.34% corrosion at the electrode site and 97.53% across the rebar, aligning with a half-cell potential of -610 mV and a very high (90%) probability of corrosion activity. The image-based results consistently reflected localized variations in corrosion severity. In samples with low electrode-based corrosion such as Sample 3 (0.74% corrosion, -187 mV), the program effectively captured the minimal spread along the rebar (4.52% corrosion overall). On the other hand, in severely deteriorated cases (e.g., Sample 19, 77.34% electrode corrosion; 85.23% total; -514 mV), the technique successfully quantified the extensive rusted regions, demonstrating robustness across both low and high corrosion ranges. Overall, across the 20 tested rebars, the algorithm exhibited quantitative corrosion values comparable to half-cell results. The confusion matrix (Figures 9–10) reinforced this finding by showing only True Positive (TP) classifications, confirming the absence of false detection errors. Importantly, the method offered spatially resolved visualizations of corroded regions, which are absent in half-cell measurements. This added layer of diagnostic detail is valuable for structural engineers, as it highlights not only the extent but also the distribution of corrosion. The slight discrepancies observed between the two methods, particularly in intermediate corrosion ranges (e.g., Samples 8–9 with 35–45% corrosion corresponding to 50% probability of activity), may be attributed to variations in surface rust visibility versus electrochemical activity. Nevertheless, the close numerical proximity demonstrates that image processing is not only suitable for qualitative detection but also capable of providing quantitative insight into corrosion progression

4. CONCLUSION

This study demonstrates that digital image processing algorithms can serve as a robust, non-destructive alternative to traditional corrosion detection methods in reinforcement bars. The proposed Python–OpenCV workflow, involving pre-processing, segmentation, thresholding, and contour analysis, achieved corrosion quantification results that closely matched those from half-cell potential testing. Key findings include:

- Detection of corrosion ranging from as low as 0.46% (Sample 1 electrode site) to as high as 97.53% (Sample 2 complete rebar), highlighting the method's versatility across different damage levels.

- A high degree of correlation with half-cell potential results, with consistent mapping of low (<200 mV), moderate (200–350 mV), and severe (>350 mV) corrosion risks.

- Perfect classification accuracy in validation, as indicated by a confusion matrix with only True Positive outputs, ensuring that the algorithm did not misidentify non-corroded regions.

- Enhanced visualization of corrosion distribution along rebars, providing engineers with more actionable insights than conventional point-based electrochemical tests.

By integrating computational precision with field validation, this approach significantly reduces subjectivity and time consumption associated with manual inspections. Furthermore, its ability to quantify and spatially locate corroded regions can aid in predictive maintenance and extend the service life of reinforced concrete structures.

In conclusion, the application of image processing techniques for corrosion detection yields results that demonstrate considerable comparability with findings obtained through the use of the half-cell potentiometer method. Through meticulous analysis and interpretation, the outcomes derived from image processing align closely with the data acquired via the traditional half-cell potential testing. The utilization of image processing algorithms, coupled with Python-based methodologies, showcases promising potential in accurately identifying and quantifying corrosion in reinforced concrete structures. The correlation between the results obtained from image processing and those acquired from the half-cell potential test signifies a notable convergence in evaluating the corrosion risk within these structures.

Moreover, the complementary nature of these methodologies enhances the accuracy and reliability of corrosion assessment. The ability to cross-reference and validate outcomes from image processing with established techniques like the half-cell potential method strengthens the credibility of the corrosion evaluation process. Such convergence consolidates confidence in the results derived from image processing, affirming its potential as a valuable tool in structural integrity assessments. Overall, the congruence between the corrosion detection outcomes obtained from image processing techniques and those derived through the half-cell potential method underlines the efficacy and reliability of employing computational approaches. This convergence signifies a step forward in adopting innovative and complementary methodologies, bolstering the assessment accuracy and aiding in the comprehensive understanding of corrosion behavior in reinforced concrete structures. Future research may expand this methodology through deep learning–based feature extraction, real-time field deployment, and integration with structural health monitoring systems. In summary, the congruence between digital image processing results and half-cell potential tests affirms the method's reliability and paves the way for its adoption in routine corrosion assessment practices.

ACKNOWLEDGEMENT

The authors express their gratitude to Department of Civil Engineering, Sharda University for providing the access to their labs for the study.

REFERENCES

1. S. Ahmad, Reinforcement corrosion in concrete structures, its monitoring and service life prediction—a review, Cem. Concr. Compos. 25 (2003) 459–471.
2. E. Alibakhshi, M. Ramezanzadeh, G. Bahlakeh, B. Ramezanzadeh, M. Mahdavian, M. Motamedi, Glycyrrhiza glabra leaves extract as a green corrosion inhibitor for mild steel in 1 M hydrochloric acid solution: Experimental, molecular dynamics, Monte Carlo and quantum mechanics study, J. Mol. Liq. 255 (2018) 185–198.
3. A.S. Amiri, E. Erdogmus, D. Richter-Egger, A comparison between ultrasonic guided wave leakage and half-cell potential methods in detection of corrosion in reinforced concrete decks, Signals 2 (2021) 413–433.
4. ASTM C876-15, Standard test method for corrosion potentials of uncoated reinforcing steel in concrete, ASTM Int. (2015).
5. S.A. Austin, R. Lyons, M.J. Ing, Electrochemical behavior of steel-reinforced concrete during accelerated corrosion testing, Corrosion 60 (2004) 203–212.
6. B. Bataineh, S.N. Abdullah, K. Omar, M. Faidzul, Adaptive thresholding methods for documents image binarization, in: Pattern Recognition: Third Mexican Conference, MCPR 2011, Cancun, Mexico, June 29–July 2, 2011, Springer, Berlin, Heidelberg, 2011, pp. 230–239.
7. D. Bradley, G. Roth, Adaptive thresholding using the integral image, J. Graph. Tools 12 (2007) 13–21.
8. Q. Cao, L. Qingge, P. Yang, Performance analysis of Otsu-based thresholding algorithms: a comparative study, J. Sens. 2021 (2021) 1–14.
9. T.Y. Goh, S.N. Basah, H. Yazid, M.J.A. Safar, F.S.A. Saad, Performance analysis of image thresholding: Otsu technique, Measurement 114 (2018) 298–307.
10. K.M.O.L. Goni, M.A. Mazumder, Green corrosion inhibitors, Corrosion Inhib. 30 (2019) 77–83.
11. Z. Niu, H. Li, Research and analysis of threshold segmentation algorithms in image processing, J. Phys. Conf. Ser. 1237 (2019) 022122.
12. P.B. Raja, M.G. Sethuraman, Natural products as corrosion inhibitor for metals in corrosive media—a review, Mater. Lett. 62 (2008) 113–116.
13. L.M. Samsu, I. Fathurrahman, Adaptive thresholding algorithms and morphological to improve the quality of Takepan Sasak image readability, J. Phys. Conf. Ser. 1539 (2020) 012031.
14. T.A. Söylev, M.G. Richardson, Corrosion inhibitors for steel in concrete: State-of-the-art report, Constr. Build. Mater. 22 (2008) 609–622.
15. İ.B. Topçu, A. Uzunömeroğlu, Properties of corrosion inhibitors on reinforced concrete, J. Struct. Eng. Appl. Mech. 3 (2020) 93–109.
16. X. Yang, X. Shen, J. Long, H. Chen, An improved median-based Otsu image thresholding algorithm, AASRI Procedia 3 (2012) 468–473.
17. J. Zheng, Y. Gao, H. Zhang, Y. Lei, J. Zhang, OTSU multi-threshold image segmentation based on improved particle swarm algorithm, Appl. Sci. 12 (2022) 11514.